Mechanisms of chromosome biorientation and bipolar spindle assembly analyzed by computational modeling

Christopher J. Edelmaier, Adam R. Lamson, Zachary R. Gergely,
Saad Ansari, Robert Blackwell, J. Richard McIntosh, Matthew A. Glaser,
and Meredith D. Betterton*

Department of Physics
University of Colorado, Boulder, CO 80309, USA
*To whom correspondence should be addressed; E-mail: mdb@colorado.edu.

Abstract

The essential functions required for mitotic spindle assembly and chromosome biorientation and segregation are not fully understood, despite extensive study. To illuminate the combinations of ingredients most important to align and segregate chromosomes in mitosis and simultaneously assemble a bipolar spindle, we developed a computational model of fission-yeast mitosis. Starting from an initial condition that mimics the onset of mitosis, the model assembles a bipolar spindle, attaches to and aligns chromosomes, corrects attachment errors, and segregates the chromosomes to the poles. The model exhibits quantitative agreement with data from fission yeast. By examining model requirements for long-lived biorientation, we find that progressive restriction of attachment geometry, destabilization of misaligned attachments, and attachment force dependence are important for robust chromosome alignment. Spindle length changes consistent with the force-balance model, and large fluctuations in spindle length can occur when the kinetochore-microtubule attachment lifetime is long. During spindle assembly, the primary spindle force generators are kinesin-5 motors and crosslinkers, while interkinetochore stretch becomes important after biorientation occurs. The same mechanisms that contribute to persistent biorientation lead to segregation of chromosomes to the poles after anaphase onset. This model therefore provides a framework to interrogate key requirements for robust chromosome biorientation, spindle length regulation, and force generation in the spindle.

Introduction

Cell biology seeks to understand how nanometer-scale molecules organize micron-scale cells, a question well-suited to theory and modeling [1]. As quantitative cell biology has grown, modeling has expanded in scope [2]. Theory and simulation can now predict cellular phenomena across length and time scales, giving new insight into cellular self-organization. In the cytoskeleton, an important challenge is understanding how a relatively small number of building blocks can produce diverse structures and machines.

Quantitative modeling has contributed to our understanding of cytoskeletal functions including mitosis [3,4], cytokinesis [5,6], and cell motility [7,8].

Chromosome segregation in eukaryotes is performed by the mitotic spindle, a self-organized microtubule (MT)-based machine [9,10]. Dynamic spindle MTs are typically organized with their plus-ends toward the center of the spindle, forming a bipolar array as the spindle poles move apart (Figure 1) [10,11]. Motor proteins and crosslinkers that bundle and slide MTs create, extend, and stabilize MT bundles (Figure 1A,B) [12–20]. As the spindle assembles, MTs attach to duplicated chromosomes at kinetochores and align them at the spindle midzone (Figure 1A-C) [21–23]. Biorientation occurs when sister kinetochores are attached to sister poles, but is often preceded by erroneous attachment (Figure 1D) [24–28]. Kinetochores therefore perform multiple functions: they link chromosomes to MTs, maintain attachment to MT ends under force and as MTs grow and shrink, sense MT attachment and tension between sisters, and regulate correction of attachment errors and the spindle-assembly checkpoint [21,29].

It is not fully understood how kinetochores, microtubules, and associated proteins robustly assemble a bipolar spindle and align chromosomes. In particular, it is unclear which kinetochore functions are most important for error correction and proper chromosome segregation [28,29]. Error correction is affected by kinetochore geometry [26,30–33] and attachment/tension sensing [21,29,34,35], although the relative contribution of different effects is not established [36–39]. Destabilization of incorrect attachments by Aurora B kinase appears to be particularly important for high-fidelity chromosome segregation [40–43]. Therefore, further insight into the minimal mechanisms required for spindle assembly and chromosome biorientation could be gained from a computational model.

Once the spindle assembles and attaches to chromosomes, it achieves a consistent length [44–48]. The force-balance model proposes that outward-directed forces from plus-end directed sliding motors separate spindle poles, while inward-directed forces from minus-end directed sliding motors and chromosomes pull the poles together [49]. This model helps explain perturbations that alter spindle length [15,46,50,51]. However, a change in spindle length may occur from a direct change in force production or from indirect effects such as alteration in MT dynamics or alignment [15,52]. In addition, the steady-state force-balance model requires extension to address spindle length fluctuations, in which the bipolar spindle assembles, but then undergoes large, dynamic length changes [50,52–58]. Computational modeling can be a valuable tool to dissect force generation and spindle length changes.

To better understand the key mechanistic requirements for chromosome biorientation and how kinetochore number and attachment affect spindle length stability, we developed a computational model of fission-yeast mitosis. *Schizosaccharomyces pombe* cells are amenable to genetic manipulation and quantitative experiments [59–63] and the spindles are small enough that full 3D simulations are computationally tractable [59,63–65]. We were motivated by previous work modeling spindle function and chromosome segregation [3,4]. Because we study de novo spindle assembly and chromosome alignment, we could not use previous models that started with an already-bipolar structure and/or chromosomes attached to the spindle. Therefore we extended a previous model of spindle assembly in the absence of chromosomes and kinetochore-microtubule attachments [63,65,66] to include chromosomes and kinetochores.

Our model successfully accomplishes spindle assembly and chromosome biorientation. The results give insight into key requirements for error correction and long-lived biorientation, emphasizing the importance of progressive restriction of attachment, destabilization of misaligned attachments, and force-dependent attachment lifetime. The turnover of kinetochore-MT attachments affects spindle mechanics, because models with larger attachment lifetime exhibit larger fluctuations in spindle length. The spindle

components which contribute most to force generation change over time: initial spindle pole separation is due to the outward force from kinesin-5 motors overcoming the passive crosslinker braking force, while interkinetochore stretch is the main inward force after biorientation. Finally, properly constructed metaphase spindles are able to robustly segregate chromosomes in the model.

Methods

Computational modeling has been used previously to study the mitotic spindle [**?**, 3, 4]. Recent work on spindle and MT organization includes studies of spindle elongation and force balance [59, 67], the formation and maintenance of antiparallel MT overlaps [68, 69], MT bundling and sliding [15], spindle movements and positioning [70, 71], spindle length and shape [15, 51, 52, 72, 73], MT organization [74], and spindle assembly from a bipolar initial condition [32, 75]. Models of kinetochore-MT attachment and biorientation have examined capture of lost kinetochores [63, 76], chromosome reorientation after MT attachment [31], attachment error correction [33, 39, 77, 78], and chromosome movement on the spindle [**?**, 52, 61, 79, 80]. Most spindle models have started with a bipolar structure or separated spindle poles, and most previous chromosome models have begun with chromosomes attached to the spindle or near a pre-formed spindle. Because we seek to model simultaneous spindle assembly and chromosome alignment with few imposed constraints, we developed a new model, building on previous work on spindle assembly in the absence of chromosomes and kinetochore-microtubule attachments [63, 65, 66].

In developing the model, we used 3-dimensional geometry and an initial condition with side-by-side centrosomes (spindle-pole bodies, or SPBs that mimics the biological configuration at the onset of mitosis. Because stochastic binding kinetics and turnover of motor proteins, crosslinkers, and kinetochore-MT attachments are important in spindle assembly and chromosome alignment, we developed methods to rapidly compute the statistical mechanics of protein binding and unbinding [63, 81–83]. The binding and unbinding of motors, crosslinkers, and kinetochore-MT attachments is microscopically reversible and force-dependent. Motor proteins move with force-dependent velocity, which can be important for force generation by crosslinking motors [63, 83]. We represent steric interactions between molecules (such as microtubules) with a hard-core short-range repulsive interaction, rather than soft repulsion. The simulations are based on Brownian dynamics, and state changes (such as motor binding/unbinding and an MT switching from growing to shrinking) are modeled using kinetic Monte Carlo [62, 63, 65, 66] (Supplementary material) (Tables S1,S2). We seek quantitative agreement between results from the simulation model and experiments, and so fix poorly constrained model parameters by direct comparison to data [63, 66].

Geometry, microtubules, motors, and crosslinkers

The simulation takes place within a sphere that represents the fission-yeast nucleus. Two SPBs are embedded in the nuclear envelope but free to move on the surface of the sphere. Each SPB nucleates 14 MTs, with their minus-ends tethered to the SPBs by a spring and which undergo dynamic instability at their plus-ends. Steric interactions mediated by short-range hard repulsion between MTs, SPBs, and the nuclear envelope (Figure 1A,B, Supplementary material).

Three classes of motors and crosslinkers assemble the spindle (Figure 1A,B). Kinesin-5 motors (representing Cut7) move bidirectionally on MTs [84–87], with plus-end directed movement on antiparallel MTs exerting force to slide apart the SPBs. Kinesin-14 motors (representing Pkl1 and Klp2)

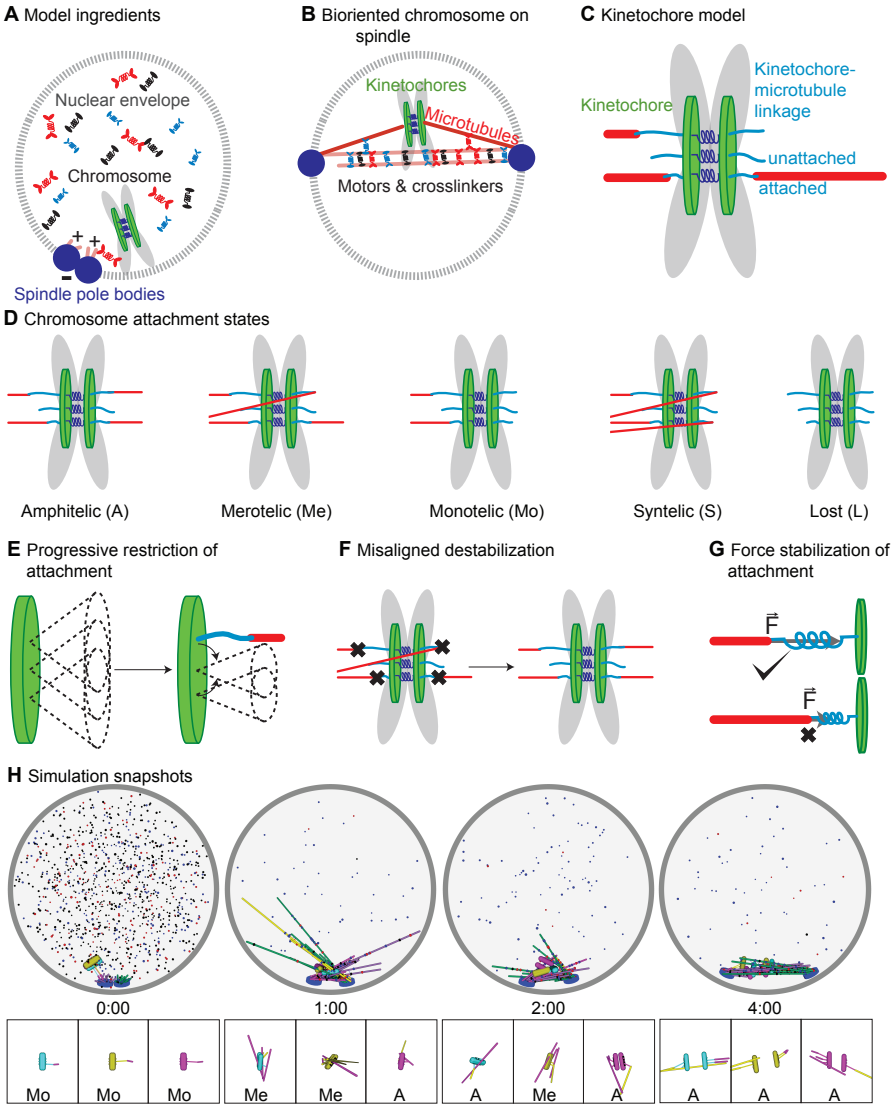

Figure 1: **Schematic of computational model and simulation of the reference model**. **(A)** Schematic of initial condition, showing adjacent spindle-pole bodies (blue) embedded in the nuclear envelope (gray dashed), proximal chromosomes (gray with green plate and blue springs), short microtubules (pink), and motor proteins and crosslinkers (red, blue, and black). **(B)** Schematic of bipolar spindle and a bioriented chromosome. **(C)** Schematic of chromosome and kinetochore model showing sister chromatids (gray), one kinetochore on each chromatid (green plates), the pericentric chromatin spring (blue springs), and kinetochore-MT attachment factor (blue line). **(D)** Schematic of chromosome attachment states, showing amphitelic, merotelic, monotelic, syntelic, and lost chromosomes. **(E)** Schematic of progressive restriction, showing that the angular range of kinetochore-MT attachment is restricted after attachment. **(F)** Schematic of misaligned destabilization of attachment, showing that misaligned attachments are destabilized. **(G)** Schematic of force stabilization of attachment, showing that end-on attachment to depolymerizing MTs has increased lifetime. **(H)** Image sequence of spindle assembly and chromosome biorientation rendered from a three-dimensional simulation. Initially, SPBs are adjacent (blue disks), MTs are short spherocylinders (green and purple when unattached to kinetochores, yellow and magenta when attached), and chromosomes (cyan, yellow, magenta) are near SPBs. Motors and crosslinkers are dispersed spots (red, blue, and black) within the nucleus (gray boundary). Time shown in minutes:seconds. Lower: a zoomed view of each chromosome with attachment state labeled.

crosslink MTs and one head walks toward the MT minus-ends, aligning MTs and exerting force that shortens the spindle [13–15, 88–91]. Crosslinkers (representing Ase1) preferentially bind antiparallel MTs [17, 18, 92–95] and stabilize MT overlaps when crosslinking near the end of an MT, an effect which mimics the recruitment of stabilizing proteins such as CLASP [53] to MT ends.

Chromosomes and kinetochores

We represent the multiple outer kinetochore proteins involved in MT binding [21, 29] by a single attachment factor that can be bound or unbound to an MT. Because fission-yeast kinetochores can bind up to 3 MTs [96], each kinetochore has 3 attachment factors in the model separated by 40 nm along the kinetochore plate (Figure 1C, Figure S1). Attachments are constrained so that no more than one attachment factor can bind to the same MT plus-end. The attachment factor is a 54-nm long spring that exerts force on the MT and kinetochore when stretched or compressed (Tables S3, S4). Attachment factors can make both lateral and end-on attachments to MTs, with different binding kinetics that favor end-on attachment. Importantly, the model includes tip tracking: a tip-bound attachment factor tracks MT ends by maintaining end-on attachment during MT growth and shrinking. The attachment factor may also include a motor, modeling kinetochore motors. End-on attachment alters MT dynamic instability and is force-dependent, as measured previously [97, 98].

Physically each kinetochore is a rectangular plate of length 150 nm, width 50 nm, and zero thickness (Figure 1C) [96] with a steric repulsion with MTs. Sister kinetochores are linked via springs that resist stretching and rotation, to maintain the distance and alignment of the kinetochores (Figure 1C, Figure S1) [**?**, 60]. The pericentric DNA is represented as a spherocylinder of length 200 nm and diameter 75 nm, which has a soft repulsion with MTs that allows MT-chromatin overlap with an energy penalty (Supplementary material).

With these ingredients, the model can achieve both correct and erroneous kinetochore-MT attachment states (Figure 1D). To achieve error correction and persistent biorientation, we found three key model ingredients were required: progressive restriction of attachment (Figure 1E), destabilization of misaligned attachment (Figure 1F), and stabilization of attachment by force (Figure 1G, Supplementary material). With these mechanisms, the model exhibits both spindle assembly and chromosome biorientation (Figure 1H, Movie S1).

Comparison to experimental results

To constrain model parameters, we developed multiple tests of simulation performance based on live-cell imaging, electron microscopy, and biorientation. First, we quantified the dynamics of spindle length and kinetochore position by confocal fluorescence light microscopy (Figure 2) [52, 63]. Cells with low-level labeling of MTs with *mCherry-atb2* [63, 99] and the *cen2-GFP* marker on the centromeric DNA of chromosome 2 [100] allowed imaging of spindle length and centromere position (Supplementary material). The Cen2 marker is displaced only 125 nm on average from the kinetochore [101], allowing quantification of the position of a single pair of sister kinetochores. We measured spindle length and kinetochore position by fitting Gaussian spots and lines to detect features, and then tracked spindle length and kinetochore position over time using previous methods (Supplementary material) [102]. Second, we used previously published electron tomographic reconstructions of fission yeast spindles [103, 104] to measure spindle structure [63]. Third, we quantified how successfully the models biorient chromosomes,

measured by the fraction of simulation time during which all the chromosomes are bioriented and the average number of end-on attachments.

We combined these measures of simulation performance in a fitness function which quantifies the overall success of any set of model parameters. We then varied poorly constrained model parameters to maximize the fitness function. The optimized parameters defined the reference model (Supplementary material).

Results

A computational model can assemble a bipolar spindle and biorient chromosomes

To understand the mechanisms most important for proper chromosome alignment on the spindle, we developed a computational model of fission-yeast mitosis (Figure 1) that includes spindle MTs nucleated from SPBs, crosslinking motors, passive crosslinkers, pericentric chromatin, and kinetochores, all contained within a spherical nucleus (Methods, Figure 1A,B). Kinetochore-MT binding occurs via attachment factors that represent MT-binding kinetochore proteins (Figure 1C), which can form both correct and erroneous MT-kinetochore attachments (Figure 1D). Kinetochore-MT attachments progressively restrict in angle as MTs bind (Figure 1E), a mechanism motivated by previous work on kinetochore geometry and chromosome rotation in error correction [26,30–33]. In particular, work on the *S. pombe* monopolin complex has proposed that monopolin acts as a site-clamp that co-orients MTs bound to the same kinetochore [30]. To correct attachment errors, we included destabilization of improper attachments and tip-enhanced catastrophe (Figure 1F), mimicking the activity of Aurora B kinase [41, 101, 105] and recapture of lost kinetochores by MT depolymerization [52, 103, 106–108]. To maintain biorientation, we implemented force-dependent kinetochore-MT attachment kinetics (Figure 1G), based on previous work that demonstrated an increase in attachment lifetime with tension when kinetochores are attached to depolymerizing MTs [97, 98]. For further details of the construction of the model, see Methods and Supplementary material. With these ingredients, the model is able to spontaneously assemble a bipolar spindle starting with side-by-side SPBs, form MT-kinetochore attachments, correct attachment errors, and biorient the chromosomes (Figure 1H, Video S1).

To refine and test the model, we measured spindle assembly and chromosome alignment in fission yeast (Figure 2, Methods, Supplementary material). We quantified spindle length, SPB-kinetochore separation, and interkinetochore stretch from the onset of mitosis until chromosome segregation (Figure 2A-D) and used these data to adjust model parameters (Methods, Supplementary material). After refinement, simulations of the reference model showed dynamics of SPB separation, kinetochore movement along the spindle, and interkinetochore stretch similar to the experimental data (Figure 2E-H, Video S2). As occurs in cells, the dynamics varied from simulation to simulation, but were similar on average (Figure 2I, Figure S2).

Single model perturbations recapitulate the requirement for kinesin-5 motors and CLASP

After developing the reference model, we verified that single model perturbations recapitulate results from fission-yeast genetics. Kinesin-5 motors are essential for spindle assembly in *S. pombe*, and temperature-sensitive mutants of the kinesin-5/Cut7 fail to separate spindle-pole bodies [91, 109–111].

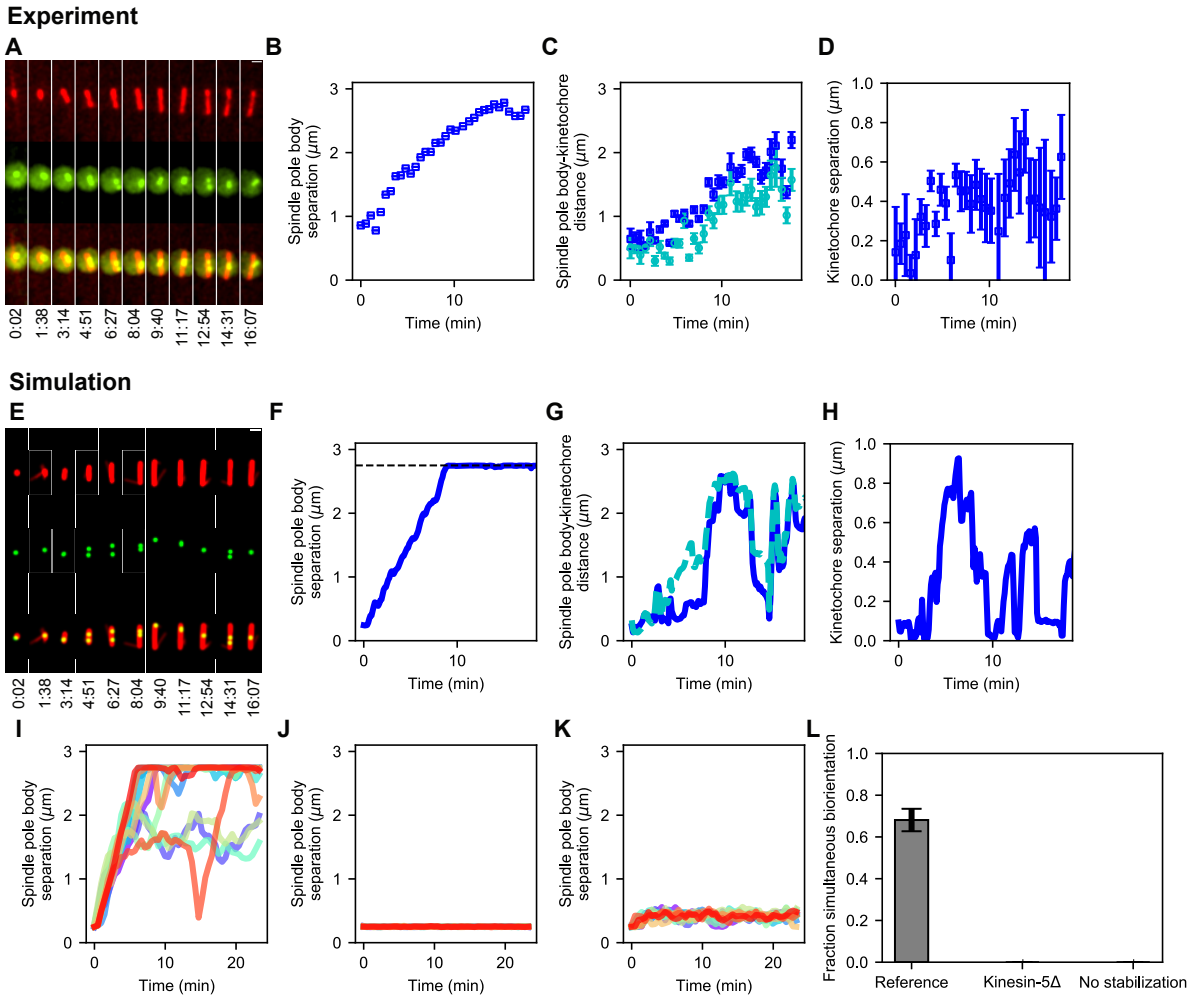

Figure 2: **Comparison of spindle assembly and chromosome alignment in cells and simulations.** **(A-D)** Experimental results. **(A)** Maximum-intensity projected smoothed images from time-lapse confocal fluorescence microscopy of fission yeast with *mCherry-atb2* labeling MTs (red) and *cen2-GFP* labeling the centromere of chromosome 2 (green). Time shown in minutes:seconds. **(B)** Spindle length, **(C)** spindle pole body-kinetochore distance, and **(D)** interkinetochore distance versus time from the experiment shown in (A). **(E-K)** Simulation results. **(E)** Simulated fluorescence microscopy images with MTs (red) and a single kinetochore pair (green). **(F)** Spindle length, **(G)** spindle pole body-kinetochore distance, and **(H)** interkinetochore distance versus time from the simulation shown in (E), sampled at a rate comparable to the experimental data in (A-D). **(I)** Spindle length versus time for 12 simulations of the reference model. **(J)** Spindle length versus time for 12 simulations in a model lacking kinesin-5. **(K)** Spindle length versus time for 12 simulations in a model lacking crosslink-mediated microtubule stabilization. **(L)** Fraction simultaneous biorientation for the reference, kinesin-5 delete, and no-stabilization models.

Consistent with this, when we remove kinesin-5 from the model, SPBs do not separate (Figure 2J). Similarly, the microtubule-associated protein CLASP is essential for spindle assembly in fission yeast, where it is recruited to MT antiparallel overlaps by Ase1 and stabilizes MT dynamics [53]. When the stabi-

lization of dynamics of crosslinked MTs is turned off in the model, SPBs do not separate (Figure 2K). Chromosome biorientation is abolished in models where the SPBs do not separate (Figure 2L, Video S2). We further studied double deletion in the simulation model (Figure S3).

Chromosome biorientation during spindle assembly requires three basic kinetochore properties

Our simulations start in a state mimicking early mitosis with monotelic chromosomes, then spontaneously assemble a bipolar spindle and biorient chromosomes. Biorientation requires the model to correct attachment errors and maintain correct attachments. This occurs in the simulations primarily through progressive restriction of attachment angle, misaligned destabilization, and force-dependent kinetochore-MT attachment.

Kinetochores can avoid merotelic attachments by progressive restriction of microtubule binding

To facilitate correct initial attachment of MTs to kinetochores, the model progressively restricts the angle at which binding can occur as more MTs bind (Figure 1E). This is motivated by previous work demonstrating that kinetochore geometry and chromosome rotation play an important role in promoting correct kinetochore-MT attachment and correcting errors [26, 30–33]. We have extended previous work to include both multiple MT binding sites per kinetochore and changes in kinetochore geometry upon binding. In our model, unattached kinetochores have a wide angular range over which attachments can form (modeled as an angular spring constant for binding, represented by the three wide cones in Figure 1E left). Each attachment formed narrows the angle allowed for the subsequent attachment, favoring attachment to MTs that are more perpendicular to the kinetochore plate (represented by the narrower cones in Figure 1E right). Attachments exert an alignment force/torque on kinetochores and MTs based on the stiffness of this angular spring.

To illustrate the importance of progressive restriction, we removed it, making the angular range identical for all three kinetochore-MT attachment events (Figure 3A, Video S3). Doing this nearly abolishes biorientation in the model: the fraction of simulation time for which all three chromosomes are bioriented is below 10%, independent the value of the angular spring constant from 1 $\mathrm{k_B T}$ (almost any angle of attachment is allowed) to 100 $\mathrm{k_B T}$ (attachment is highly restricted in angle). These failures occur for different reasons as the angular spring constant varies. When attachment angle is most permissive, merotelic attachments form and are not corrected sufficiently rapidly to biorient the chromosomes. When the attachment angle is highly restricted, attachments are unlikely to form at all. Overall, this result shows that in our model progressive restriction of attachment is essential for biorientation.

The progressive restriction model requires that the first binding event be relatively permissive in angle, the second more restricted, and the third highly restricted. To study this, we varied the angular spring constant of each attachment independently (Figure 3B,C, Figure S4, Video S3). The model achieves a high fraction of simultaneous biorientation around 70% when the first attachment is maximally permissive (spring constant is 1 $\mathrm{k_B T}$); an increase in this spring constant restricts the angle and decreases simultaneous biorientation to below 20% (Figure 3B). This means that for the first attachment, promoting kinetochore binding to any MT is important: initial attachments should be established easily, even if erroneous. By contrast, biorientation is increased when the third (final) binding event is highly restricted (Figure 3C): chromosomes are bioriented in the model $<$10% of the time when the third attachment is

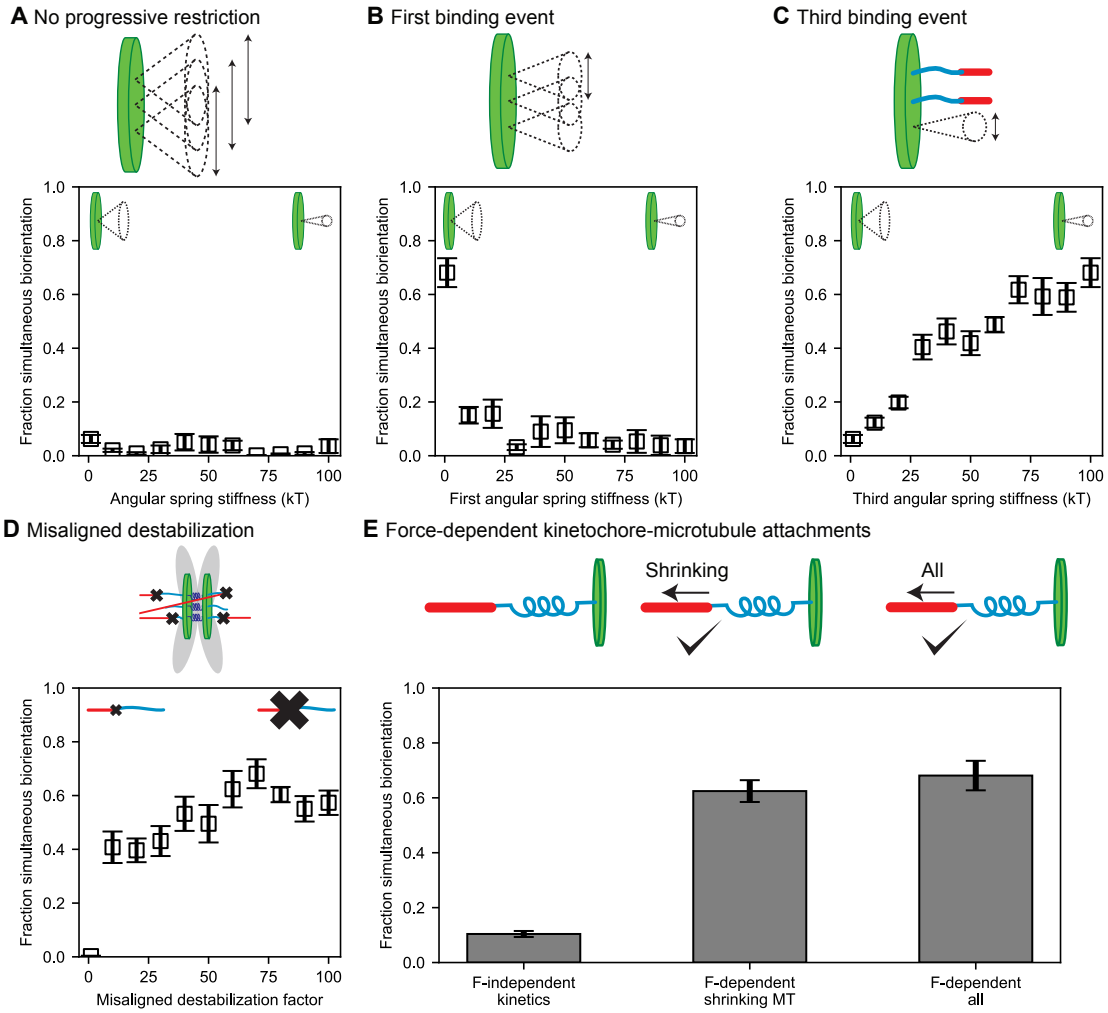

Figure 3: **Results of perturbing kinetochore properties required for biorientation**. **(A)** Fraction simultaneous biorientation versus angular spring stiffness in models lacking progressive restriction of attachment. **(B)** Fraction simultaneous biorientation versus the first angular spring stiffness in the model with progressive restriction. **(C)** Fraction simultaneous biorientation versus the third angular spring stiffness in the model with progressive restriction. **(D)** Fraction simultaneous biorientation versus the misaligned destabilization factor. **(E)** Fraction simultaneous biorientation for different types of force-dependent kinetics.

most permissive, but the fraction of simultaneous biorientation increases with the angular stiffness of the third binding site.

Because of the importance of progressive restriction in our model, we additionally examined whether varying the number of allowed kinetochore-MT attachments might affect how easily biorientation is achieved, but found no significant effect (Figure S4).

Error correction occurs through the destabilization of improper attachments

Progressive restriction of attachment reduces but does not eliminate erroneous kinetochore-MT attachments. Previous experimental work has shown that merotelic attachments are common in early mitosis and are corrected over time [112] due to increased turnover of kinetochore MTs from the activity of Aurora B kinase [41,101,105]. We implemented misaligned destabilization in the model by accelerating the detachment of kinetochore-MT attachments that are not amphitelic (Figure 1F). Because experimental work has demonstrated a decrease in kinetochore MT turnover by up to a factor of 65 in the presence of Aurora B inhibitors [41], we varied the misaligned destabilization factor in the model, which quantifies the increased turnover of incorrect attachments, over a similar range from 1 to 100 (Figure 3D, Video S3). Consistent with experimental results, biorientation is nearly eliminated in the absence of misaligned destabilization. Biorientation time in the model is maximum when the misaligned destabilization factor is 70, comparable to the experimental value. This demonstrates the importance of error correction in the model.

Persistent biorientation is achieved through force-dependent kinetochore-microtubule attachment

Once amphitelic kinetochore-MT attachments are formed, they must be maintained for biorientation to persist. Micromanipulation experiments have demonstrated that increasing force on chromosomes can stabilize their attachment to spindle MTs [113]. Attachments between single MTs and purified budding-yeast kinetochores were altered by force applied to the kinetochore, even in the absence of Aurora kinase [97,98]. In particular, the kinetochore-MT attachment lifetime increased with tension when kinetochores were attached to depolymerizing MTs, an effect dependent on a TOG protein [97, 98]. Consistent with this, we implemented force dependence of attachments in the model (Figure 1G). This effect is required to maintain biorientation: if we eliminate the force dependence of attachment kinetics, biorientation is nearly abolished in the model (Figure 3E, Video S3). To understand which force-dependent rate is most important for this effect, we added them back to the model one at a time. The increase in attachment lifetime of a kinetochore bound to a shrinking MT is the key force-dependent rate, because making this the only force-dependent lifetime in the model restores nearly all biorientation compared to the model with all rates force-dependent (Figure 3E). This demonstrates that maintenance of biorientation requires kinetochore-MT attachments to persist during MT depolymerization.

Slow turnover of kinetochore-microtubule attachments can cause spindle length fluctuations

Spindle length regulation [15, 44–47, 50] can be understood using the force-balance model of Saunders and Hoyt in which plus-end directed sliding motors produce outward force, and minus-end directed sliding motors and chromosomes produce inward force [49, 50, 114–123]. The force-balance model has been used in mathematical models of spindles in yeast [15, 51, 59, 63, 65, 66, 124, 125], and *Drosophila* [126–129] cells. This work has focused on spindle length at steady state, not dynamic changes. However, some fission-yeast mutants exhibit large fluctuations in spindle length in which the bipolar spindle assembles, but then shortens or falls apart, known as spindle collapse [50, 52–58]. Remarkably, fission-yeast double mutants can have wild-type average metaphase spindle length, but much larger fluctuations than wild-type [50]. The underlying mechanisms of large spindle length fluctuations have remained unclear, in part because apparently contradictory changes can cause it. For example,

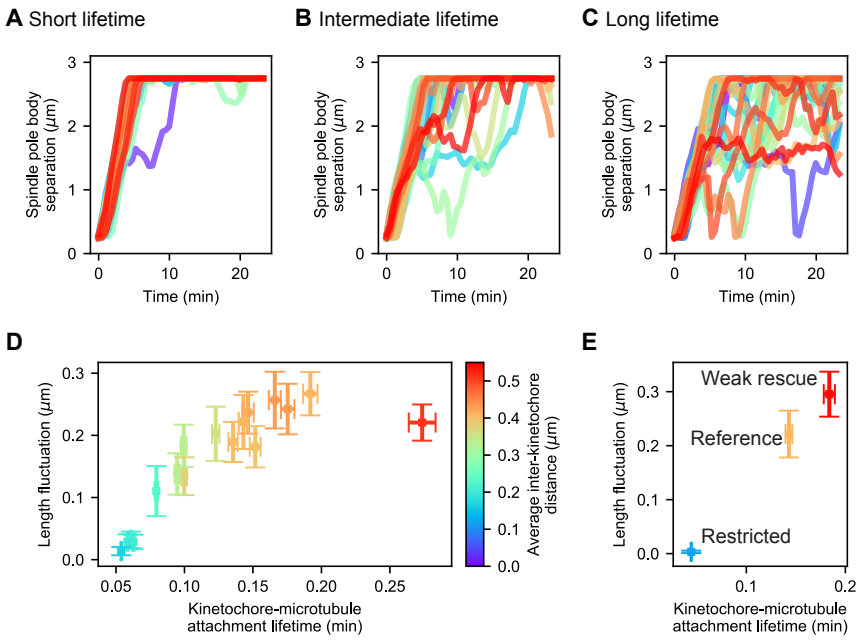

Figure 4: **Changes in kinetochore-MT attachment turnover alter spindle length fluctuations.** **(A-C)** Spindle length versus time for 12 simulations of the same model, with **(A)** short (1/4 the reference value), **(B)** intermediate (1/2 the reference value), and **(C)** long (twice the reference value) kinetochore-MT attachment lifetime. **(D)** Length fluctuation magnitude versus measured kinetochore-MT attachment lifetime and average interkinetochore stretch (color) for bioplar spindles (corresponding to simulation time >10 min.). **(E)** Length fluctuation magnitude versus measured kinetochore-MT attachment lifetime and average interkinetochore stretch (color) for the reference, restricted, and weak rescue models.

deletion of proteins known either to stabilize [53] or destabilize MTs [52] can both lead to large spindle length fluctuations. In recent work we examined how deletion of the kinesin-8 motor proteins could contribute to large spindle length fluctuations in fission yeast [52], but a general understanding of this phenomenon is unknown. Therefore, we sought to understand what spindle functions might lead to large length fluctuations.

One key determinant of the magnitude of spindle length fluctuations is the lifetime of kinetochore-MT attachments (Figure 4, Video S4). We quantified the magnitude of length fluctuations by determining the standard deviation in spindle length over time after spindle elongation for each individual simulation of the model, then averaging that standard deviation over multiple model runs with the same parameters. This measure of length fluctuations varies linearly with kinetochore-MT attachment lifetime: the longer the lifetime, the larger the fluctuations (Figure 4A-D).

To understand this result, we hypothesized that for long-lived attachment, the force exerted by a stretched kinetochore can grow over time to a larger value: long-lived attachment allows multiple MTs to bind per kinetochore, exert greater force, and stretch apart the sisters. This allows larger inward force to be exerted on the spindle by attached kinetochores. Indeed, the average interkinetochore distance increases with kinetochore-MT attachment lifetime (Figure 4D). Thus, slow cycles of attachment and detachment lead to slowly varying force on the spindle that causes its length to fluctuate. In the opposite

limit, short-lived kinetochore-MT attachment causes relatively quick turnover, limiting interkinetochore stretch, inward force, and variation in inward force.

Alteration in kinetochore-MT attachment lifetime could occur through multiple molecular mechanisms. To illustrate how this could occur, we considered two perturbations to the model that have downstream effects on both lifetime and length fluctuations (Figure 4E). The first perturbation is a restricted attachment model, in which the angular spring constant of attachment discussed above (Figure 3A) is set to 100 $\mathrm{k_B T}$ for all attachments. In this case attachments rarely form and when formed, their lifetime is short (< 0.05 min on average). As a result, the force produced by interkinetochore stretch is small and does not vary much, leading to small length fluctuations in the model (< 0.01 μm on average). The opposite limit can occur in a model in which the force-dependent rescue of kinetochore MTs is greatly reduced, by increasing the force constant from 6.4 pN to 12.8 pN (this reduces the force sensitivity of rescue, see Supplementary material). This causes kinetochore MTs to depolymerize for longer time, and because kinetochore-MT attachments are stabilized during depolymerization, this change dramatically increases the attachment lifetime to 0.2 min. As a result, interkinetochore stretch can increase, and length fluctuations correspondingly increase (0.2 μm).

This analysis suggests that altered kinetochore-MT attachment lifetime could be a downstream effect that results from some of the diverse mutations observed to cause spindle length in *S. pombe*. We note that the effect of lifetime may not be the only source of spindle length fluctuations: other mutations that lead to slow changes in force exerted on the spindle could have similar effects.

Force generation in the spindle varies during spindle elongation

The force-balance model can explain why multiple perturbations alter steady-state spindle length, including mutation of motors and microtubule-associated proteins [15, 50], and chromosome/kinetochore number and chromatin stiffness [46, 51]. However, it can be challenging to distinguish direct from indirect effects of altering force balance. For example, the force-balance model posits that minus-end-directed kinesin-14 motors contribute inward force that shortens the spindle, so their deletion would be expected to lead to longer spindles. However, in budding yeast, kinesin-14 deletion instead leads to shorter spindles, because kinesin-14 helps bundle spindle MTs, allowing kinesin-5 motors to generate greater outward force when kinesin-14 is present [15]. Similarly, kinesin-8 deletion in fission yeast leads to longer spindles, but this is likely due to effects of this motor on MT dynamics rather than direct inward force generation by kinesin-8 [50, 52].

To better understand direct and indirect changes in spindle length, we examined the force produced by spindle molecules as the spindle elongates, averaged over many simulation runs (Figure 5, Video S5). In this analysis, we considered each half-spindle separately, and calculated the total force exerted along the spindle axis produced by separate force-generating elements: outward force by kinesin-5 motors, and inward force by kinesin-14 motors, passive crosslinkers, and kinetochore-MT attachments (Figure 5A). We computed spindle length as a function of time (Figure 5B,E,H), force as a function of time (Figure 5C,F,I) and spindle length (Figure 5D,G,J) in the reference, restricted attachment, and weak rescue models.

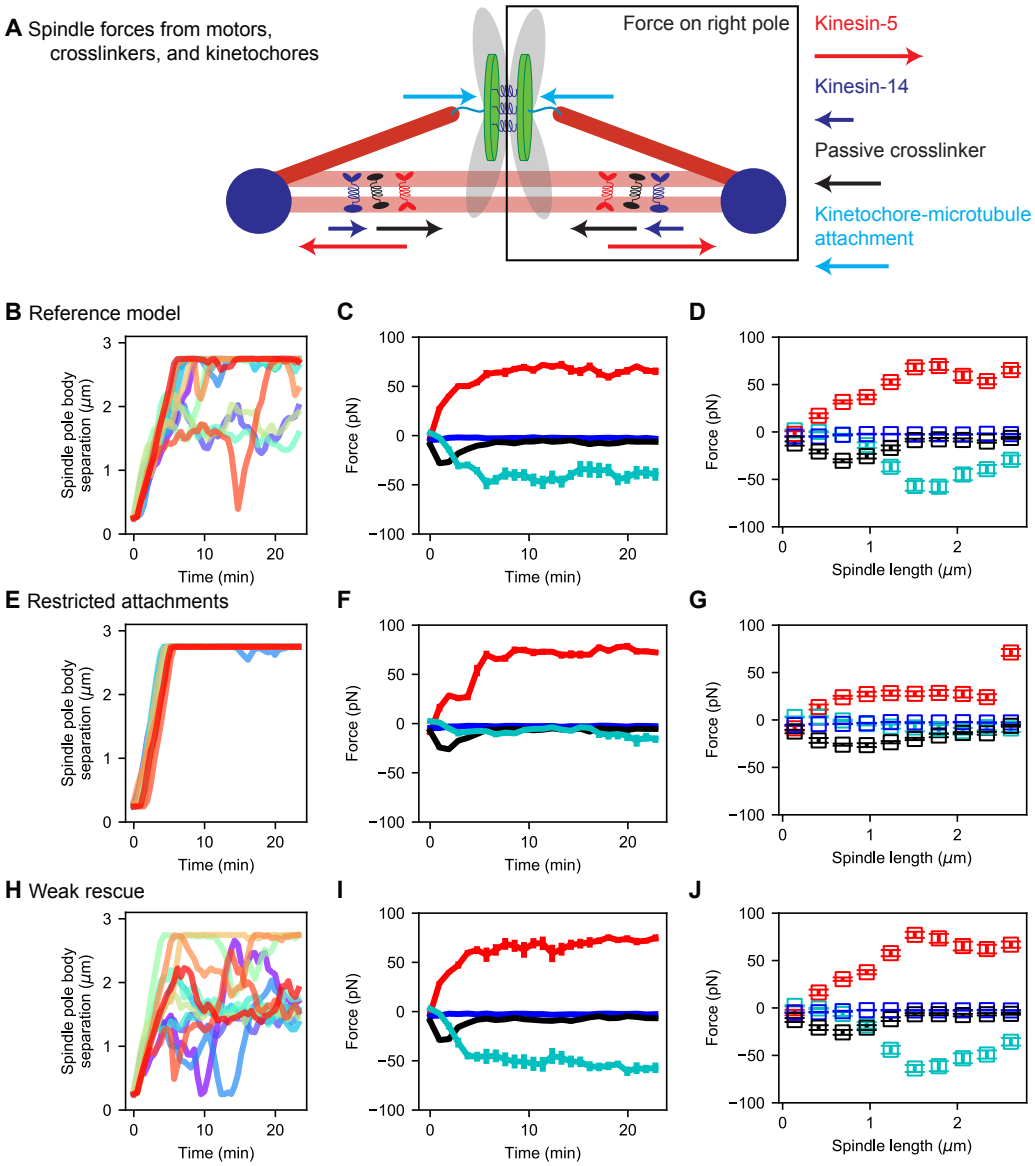

Figure 5: **Spindle force generation varies as the spindle assembles and elongates.** **(A)** Schematic of force generation along the spindle axis, showing kinesin-5 motors exerting outward force (red) and kinesin-14 (dark blue), crosslinkers (black), and kinetochore-MT attachment to stretched chromosomes (light blue) exerting inward force. **(B, E, H)** Spindle length versus time, **(C, F, I)** average spindle axis force versus time, and **(D, G, J)** average spindle axis force versus spindle length for three different models: **(B-D)** the reference model, **(E-G)** the restricted attachment model, and **(H-J)** the weak rescue model.

The early bipolar spindle forms due to motors and crosslinkers, not chromosomes

Force generation by kinesin-5 motors, kinesin-14 motors, crosslinkers, and chromosomes changes significantly as the bipolar spindle assembles. For early time (up to 5 minutes) when spindles are short

(up to 1 μm), motors and crosslinkers exert force that slowly increases in magnitde up to a few tens of pN, but chromosomes exert almost no force (Figure 5C,F,I, Video S5). Because chromosomes are not bioriented on the spindle during initial SPB separation, they do not exert significant inward force. This result is consistent with our previous work, which demonstrated that initial bipolar spindle assembly can occur in a model lacking chromosomes [63, 65, 66].

The outward sliding force produced by kinesin-5 motors increases approximately linearly with spindle length, as the length of antiparallel MT overlaps increases during spindle assembly (Figure 5D,G,J). This agrees with the experimental result that the sliding force generated by kinesin-5 motors is proportional to overlap length [130]. The inward force generated by kinesin-14 motors is small, as in previous work that has shown that kinesin-14 is less effective at force generation that kinesin-5 [131] and that in the spindle kinesin-14 may be more important to align spindle MTs than to generate force directly [15].

During initial spindle assembly, crosslinkers play the primary role in maintaining antiparallel MT overlaps in opposition to the sliding activity of kinesin-5. Remarkably, we find that the inward force generated by passive crosslinkers initially increases with spindle length to approximately 25 pN when the spindle is 0.75 μm long. Beyond this point, the crosslinker force steadily decreases, dropping to near zero within a few minutes (Figure 5C,F,I). This is consistent with previous results on force generation by the crosslinker Ase1, which found large force for small overlaps that drops significantly as overlaps become larger [20]. Therefore, our results support a picture of early spindle assembly in which high braking force by crosslinkers on short antiparallel MT overlaps oppose the outward force generated by kinesin-5. This highlights the key role of crosslinkers in early spindle assembly seen previously [63, 65, 66].

Metaphase spindle length is determined primarily by interkinetochore stretch and kinesin-5 motors

Once the spindle elongates sufficiently to separate SPBs by 1 μm, there is a transition in the primary contributer to spindle force. In this regime, chromosomes biorient and the inward force from interkinetochore stretch becomes significant, balancing outward force from kinesin-5 motors (Figure 5C,F,I). This balance is crucial to setting metaphase spindle length.

To perturb this force balance, we considered two additional models discussed above (Figure 4E) with restricted attachment and weak rescue. When attachment is restricted, chromosomes rarely biorient and the inward force from chromosomes is small for spindles of all length. This leads to unbalanced force from kinesin-5 motors and long spindles (Figure 5E-G, Video S5). When MT rescue is reduced, interkinetochore stretch is larger and the inward force from stretched sister kinetochores increases (Figure 5H-J, Video S5). This leads to shorter metaphase spindle length and a corresponding increase in force from stretched kinetochores.

Chromosome segregation can occur via the same mechanisms that assemble the spindle

After developing the model of spindle assembly and chromosome biorientation, we examined what additional mechanisms were required for the model to segregate chromosomes to the poles. Relatively few changes are required for robust chromosome segregation, suggesting that significant new mechanisms are not required in anaphase for chromosome segregation. The rules added to the model for anaphase A include severing the chromatin spring between kinetochores (based on cumulative time the chromosomes are bioriented), stabilization of kinetochore-MT attachment, and depolymerization of MTs (Table

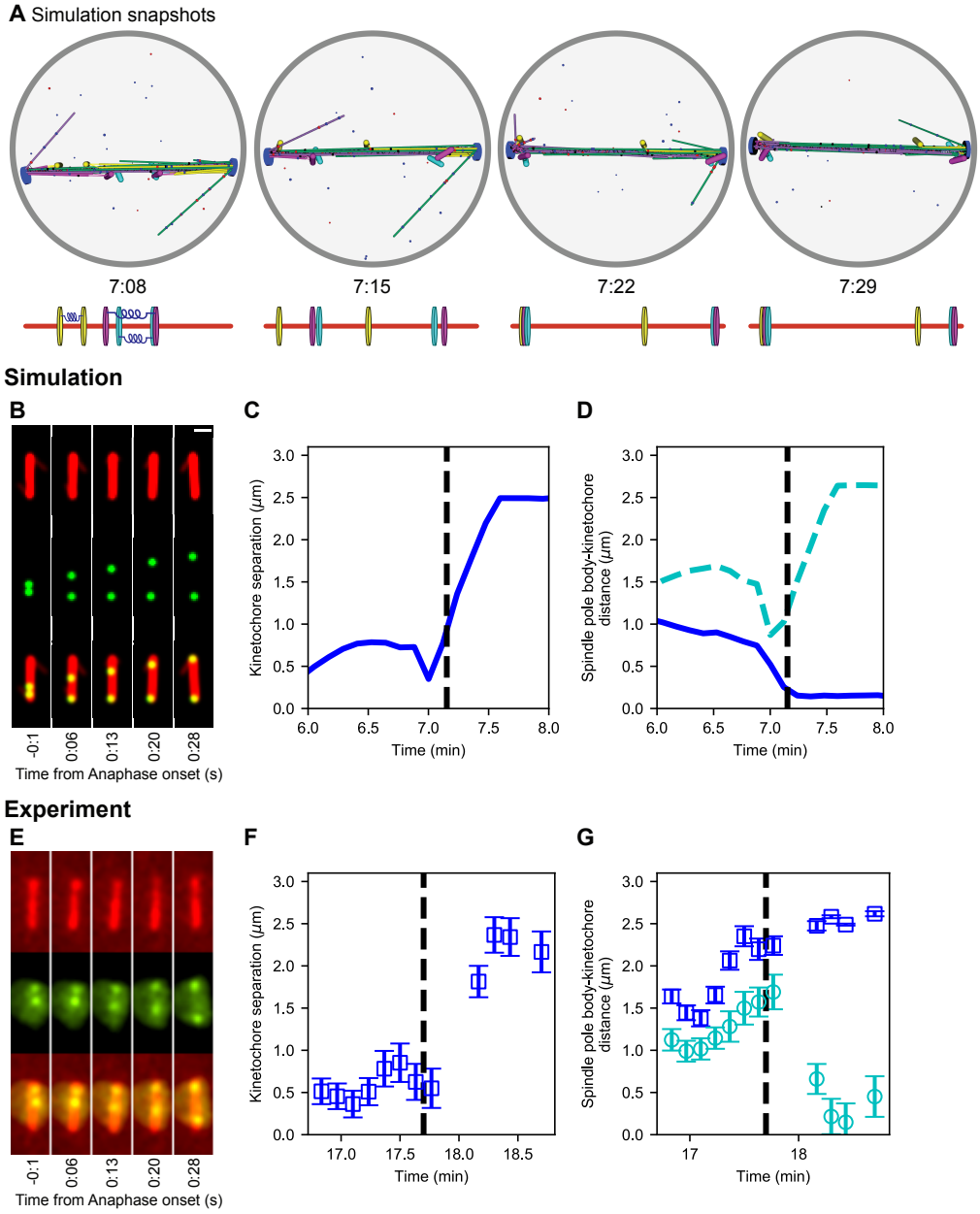

Figure 6: **Chromosome segregation in the model and comparison to experiments**. **(A)** Image sequence of simulation of chromosome segregation after anaphase is triggered, rendered from a three-dimensional simulation. Anaphase begins immediately after the first image. Lower, schematic showing kinetochore position along the spindle. Time shown in minutes:seconds. **(B-D)** Simulation results. **(B)** Simulated fluorescence microscopy images with MTs (red) and a single kinetochore pair (green). Time shown in minutes:seconds. **(C)** Spindle pole body-kinetochore distance, and **(D)** interkinetochore distance versus time from the simulation shown in (B), sampled at a rate comparable to the experimental data in (E-G). **(E-G)** Experimental results. Maximum-intensity projected smoothed images from time-lapse confocal fluorescence microscopy of fission yeast with *mCherry-atb2* labeling MTs (red) and *cen2-GFP* labeling the centromere of chromosome 2 (green). Time shown in minutes:seconds. **(E)** Spindle length, **(F)** spindle pole body-kinetochore distance, and **(G)** interkinetochore distance versus time from the experiment shown in (E).

S5). With these additions to the model, simulations consistently segregate chromosomes to the poles (Figure 6A-D, Video S6). We compared our simulations to experimental measurements of chromosome segregation, and found similar speed of chromosome movement to the poles and separation of sisters (Figure 6E-G).

Discussion

The computational model of mitosis presented here can biorient chromosomes as the spindle assembles. This framework allows us to examine which functions are most important to assemble a bipolar spindle, attach kinetochores to spindle MTs, biorient chromosomes, and segregate them to the poles (Figure 1, Video S1). Our model was refined with experimental data on spindle structure, spindle elongation, and chromosome movements in fission yeast, leading to quantitative agreement with the data (Figure 2, Video S2). The reference model results match previous genetics that found that kinesin-5 motors and CLASP are essential for bipolar spindle assembly [53, 63, 109, 110], which suggests that the model captures key features needed to provide insight into mitotic mechanism.

Three ingredients are required for long-lived biorientation in the model (Figure 3, Video S3). Kinetochores shield themselves from merotely by progressive restriction of attachment. Inclusion of this effect in the model was motivated by recent work on the monopolin complex in fission yeast [30] and attachment-driven compaction of mammalian kinetochores [32]. Progressive restriction has two key effects: it promotes proper attachment by favoring binding of microtubules from the same pole that is already attached to the kinetochore, and simultaneously creates a torque that helps to reorient the kinetochore on the spindle. In previous work, the monopolin complex components Pcs1/Mde4 were found not to be essential in fission yeast [30], but in our model completely removing progressive restriction abolishes biorientation (Figure 3). This suggests the possibility that in fission yeast, other molecules may contribute to progressive restriction in addition to monopolin.

Mimicking the effects of Aurora B kinase by including destabilization of misaligned attachments allows the model to achieve robust error correction. Destabilization by approximately a factor of 70 gives the highest degree of biorientation the model. This is similar to the degree of destabilization previously estimated to occur due to Aurora B [41], further suggesting that the model produces biologically relevant results.

To maintain long-lived biorientation in the model, kinetochore-MT attachment lifetime must increase with tension during microtubule depolymerization. This catch-bond behavior has been previously measured for purified budding-yeast kinetochores attached to single microtubules [97, 98]. Without this force dependence, kinetochores frequently detach from depolymerizing MTs and lose biorientation. Our model achieves biorientation for the longest time with an increased force-sensitivity of attachment compared to experimental measurements, a difference that would be of interest to explore in future work.

The timing of spindle assembly and biorientation in the model were consistent with those quantified experimentally. A current difference between the model and experiment is that we find ongoing turnover of kinetochore-MT attachments, so that biorientation can be lost once established. This is in contrast to previous experimental work, which suggests that for metaphase spindles, once biorientation is established it is rarely lost [39, 132, 133]. The mechanisms underlying this difference are an open question.

Using our model, we studied the origins of large spindle length fluctuations (Figure 4, Video S4).

While previous work has examined regulation of spindle length [15, 46, 47, 50], what mechanisms might drive large fluctuations in spindle length over time have been less well-studied. We identified the lifetime of kinetochore-MT attachment as a determinant of the degree of spindle length fluctuations. Long attachment lifetime allows bioriented chromosomes to become more stretched, leading to large, slowly varying inward force on the spindle. Our results suggest why large spindle length fluctuations have not been seen in larger spindles in vertebrate cells: in *S. pombe*, a relatively small number of kinetochores and MTs contribute to spindle length, and therefore the changing force on the three chromosomes can have a significant effect on the spindle. In vertebrate spindles with tens of thousands of MTs, changes in force on a small number of kinetochores contribute only a small fractional change to overall force on the spindle, leading to smaller fluctuations.

To understand how force generation changes as the spindle assembles, we quantified the force generated by different classes of spindle molecule (Figure 5, Video S5). The early spindle has almost no force generation from interkinetochore stretch because chromosomes are rarely bioriented at this stage. Instead, the early spindle is characterized by outward force from kinesin-5 motors that is resisted by crosslinkers. Consistent with earlier work [20], the force from crosslinkers is highest when MT antiparallel overlaps are short and drops as the spindle elongates. Once the bipolar spindle is formed and chromosomes are bioriented, attached chromosomes provide significant inward force that opposes the outward force of kinesin-5 motors. These results suggest that the many mutations that alter spindle length in fission yeast [50] might act indirectly by altering kinesin-5 force generation or interkinetochore stretch.

Remarkably, the model is able to transition to anaphase A and robustly segregate chromosomes to the poles with a small number of additional rules (Figure 6, Video S6). Overall, our work provides a powerful framework for testing spindle assembly mechanisms that can inform future experimental studies.

Acknowledgments

We thank Jeffrey K. Moore for useful discussions. This work was funded by NSF grants DMR1725065 (MDB), DMS1620003 (MAG and MDB), and DMR1420736 (MAG); NIH grants K25GM110486 (MDB), R01GM124371 (MDB); a fellowship provided by matching funds from the NIH/University of Colorado Biophysics Training Program (AL); and use of the Summit supercomputer, supported by NSF grants ACI1532235 and ACI153223.

Supplementary movies

Movie S1

Simulation of reference model shows spindle assembly simultaneous with chromosome biorientation. Initially short MTs begin to grow at the start of the simulation and interact with nearby kinetochores. A bipolar spindle forms as the chromosomes begin to biorient. Finally, a metaphase spindle is established with bioriented chromosomes that move along the spindle and breathe. The insets are zoomed views of each chromosome, showing attachment turnover and interkinetochore stretch.

Movie S2

Top: Simulation of reference model (left) and simulated fluorescence microscopy images (right), with red MTs and green kinetochore (scale bar 1 μm). The simulated fluorescence images are rotated so that the spindle is vertical. Lower: simulation of models mimicking genetic perturbation. Lower left: Model lacking kinesin-5 motors. The SPBs never separate and the spindle remains monopolar. Chromosomes do not biorient. Lower right: Model lacking crosslinker-mediated stabilization of MT dynamics. SPBs separate only slightly, forming a short spindle that is nearly indistinguishable from a monopolar spindle. Chromosomes do not biorient.

Movie S3

Simulations of models with perturbation to kinetochore properties important for biorientation. Top left: Model lacking progressive restriction, with a permissive angular spring stiffnesses of 1 $\mathrm{k_B T}$ for all attachments. A short bipolar spindle forms, but chromosomes are typically merotelically attached and do not biorient. Top middle: Model lacking progressive restriction, with a restricted angular spring stiffnesses of 100 $\mathrm{k_B T}$ for all attachments. A long bipolar spindle forms, kinetochore-MT attachments are transient, and chromosomes do not generate significant inward force on the spindle. Top right: Model including progressive restriction but with a restricted angular spring stiffness of 20 $\mathrm{k_B T}$ for the first binding event. A long bipolar spindle forms, and kinetochore-MT attachments are transient. Lower left: model including progressive restriction but with a permissive angular spring stiffness of 20 $\mathrm{k_B T}$ for the third binding event. Error correction is impaired, and chromosomes are typically merotelically attached. Lower middle: Model lacking misaligned destabilization. Error correction is impaired. Lower right: Model with force-independent attachment kinetics. Kinetochore-MT attachments are not stabilized under tension from depolymerizing microtubules, leading to short-lived biorientation.

Movie S4

Simulations of models with varying kinetochore-MT attachment lifetime. Left: Model with short attachment lifetime in which the kinetochore-MT binding and unbinding rates are 4 times larger than in the reference model. Biorientation is somewhat compromised. Middle: Model with intermediate attachment lifetime in which the kinetochore-MT binding and unbinding rates are 2 times larger than in the reference model. Right: Model with long attachment lifetime in which the kinetochore-MT binding and unbinding rates are 2 times smaller than in the reference model. Biorientation is preserved and the spindle undergoes large length fluctuations.

Movie S5

Simulations of reference, restricted, and weak rescue models. Left: The reference model shows typical spindle length fluctuations. Middle: The restricted attachment model shows minimal length fluctuations, because transient kinetochore-MT attachments lead to low inward force on the spindle from chromosomes. Right: The weak rescue model shows large spindle length fluctuations, because kinetochore MTs remain attached while depolymerizing, leading to high and fluctuating inward force on the spindle from chromosomes.

Movie S6

Simulations of anaphase chromosome segregation. Anaphase occurs at 7:09. Top: Simulation movie showing that separation of the sister chromatids occurs after 4.45 minutes of the simultaneous biorientation of all three chromosomes. The zoomed views show the chromosomes achieving this biorientation, before segregating to the spindle poles. Lower: Simulation movie (left) and simulated fluorescence microscopy images (right), with red MTs and green kinetochore (scale bar 1 μm). The simulated fluorescence images are rotated so that the spindle is vertical.

References

[1] Wallace F. Marshall. Introduction to Quantitative Cell Biology. Colloquium Series on Quantitative Cell Biology, 3(1):i–50, July 2017.

[2] Alex Mogilner, Roy Wollman, and Wallace F. Marshall. Quantitative Modeling in Cell Biology: What Is It Good for? Developmental Cell, 11(3):279–287, September 2006.

[3] A. Mogilner and E. Craig. Towards a quantitative understanding of mitotic spindle assembly and mechanics. Journal of Cell Science, 123(20):3435–3445, 2010.

[4] Gul Civelekoglu-Scholey and Daniela Cimini. Modelling chromosome dynamics in mitosis: A historical perspective on models of metaphase and anaphase in eukaryotic cells. Interface Focus, 4(3):20130073, June 2014.

[5] Matthew Akamatsu, Julien Berro, Kai-Ming Pu, Irene R. Tebbs, and Thomas D. Pollard. Cytokinetic nodes in fission yeast arise from two distinct types of nodes that merge during interphase. J Cell Biol, 204(6):977–988, March 2014.

[6] Matthew R. Stachowiak, Caroline Laplante, Harvey F. Chin, Boris Guirao, Erdem Karatekin, Thomas D. Pollard, and Ben O'Shaughnessy. Mechanism of Cytokinetic Contractile Ring Constriction in Fission Yeast. Developmental Cell, 29(5):547–561, June 2014.

[7] Jun Allard and Alex Mogilner. Traveling waves in actin dynamics and cell motility. Current opinion in cell biology, 25(1):107–115, February 2013.

[8] Erin L. Barnhart, Jun Allard, Sunny S. Lou, Julie A. Theriot, and Alex Mogilner. Adhesion-Dependent Wave Generation in Crawling Cells. Current Biology, 27(1):27–38, January 2017.

[9] D. Bray. Cell Movements: From Molecules to Motility. Routledge, 2000.

[10] J. Richard McIntosh, Maxim I. Molodtsov, and Fazly I. Ataullakhanov. Biophysics of mitosis. Quarterly Reviews of Biophysics, 45(02):147–207, 2012.

[11] Edwin W. Taylor. Dynamics of Spindle Formation and Its Inhibition by Chemicals. The Journal of Biophysical and Biochemical Cytology, 6(2):193–196, January 1959.

[12] Barbara J. Mann and Patricia Wadsworth. Kinesin-5 Regulation and Function in Mitosis. Trends in Cell Biology, September 2018.

[13] A L Pidoux, M LeDizet, and W Z Cande. Fission yeast pkl1 is a kinesin-related protein involved in mitotic spindle function. Molecular Biology of the Cell, 7(10):1639–1655, October 1996.

[14] Chun Ju Chen, Ken Porche, Ivan Rayment, and Susan P. Gilbert. The ATPase Pathway That Drives the Kinesin-14 Kar3Vik1 Powerstroke. Journal of Biological Chemistry, 287(44):36673–36682, October 2012.

[15] Austin J. Hepperla, Patrick T. Willey, Courtney E. Coombes, Breanna M. Schuster, Maryam Gerami-Nejad, Mark McClellan, Soumya Mukherjee, Janet Fox, Mark Winey, David J. Odde, Eileen O'Toole, and Melissa K. Gardner. Minus-End-Directed Kinesin-14 Motors Align Antiparallel Microtubules to Control Metaphase Spindle Length. Developmental Cell, 31(1):61–72, October 2014.

[16] Christina L. Hueschen, Vahe Galstyan, Meelad Amouzgar, Rob Phillips, and Sophie Dumont. Microtubule End-Clustering Maintains a Steady-State Spindle Shape. Current Biology, 29(4):700–708.e5, February 2019.

[17] Akira Yamashita, Masamitsu Sato, Akiko Fujita, Masayuki Yamamoto, and Takashi Toda. The Roles of Fission Yeast Ase1 in Mitotic Cell Division, Meiotic Nuclear Oscillation, and Cytokinesis Checkpoint Signaling. Molecular Biology of the Cell, 16(3):1378–1395, January 2005.

[18] Marcel E. Janson, Rose Loughlin, Isabelle Loïodice, Chuanhai Fu, Damian Brunner, François J. Nédélec, and Phong T. Tran. Crosslinkers and Motors Organize Dynamic Microtubules to Form Stable Bipolar Arrays in Fission Yeast. Cell, 128(2):357–368, January 2007.

[19] Marcus Braun, Zdenek Lansky, Gero Fink, Felix Ruhnow, Stefan Diez, and Marcel E. Janson. Adaptive braking by Ase1 prevents overlapping microtubules from sliding completely apart. Nature Cell Biology, 13(10):1259–1264, 2011.

[20] Zdenek Lansky, Marcus Braun, Annemarie Lüdecke, Michael Schlierf, Pieter Rein ten Wolde, Marcel E. Janson, and Stefan Diez. Diffusible Crosslinkers Generate Directed Forces in Microtubule Networks. Cell, 160(6):1159–1168, March 2015.

[21] Andrea Musacchio and Arshad Desai. A Molecular View of Kinetochore Assembly and Function. Biology, 6(1):5, January 2017.

[22] Stephen M. Hinshaw and Stephen C. Harrison. Kinetochore Function from the Bottom Up. Trends in Cell Biology, 28(1):22–33, January 2018.

[23] Grace Hamilton, Yoana Dimitrova, and Trisha N. Davis. Seeing is believing: Our evolving view of kinetochore structure, composition, and assembly. Current Opinion in Cell Biology, 60:44–52, October 2019.

[24] Daniela Cimini, Bonnie Howell, Paul Maddox, Alexey Khodjakov, Francesca Degrassi, and E. D. Salmon. Merotelic Kinetochore Orientation Is a Major Mechanism of Aneuploidy in Mitotic Mammalian Tissue Cells. The Journal of Cell Biology, 153(3):517–528, April 2001.

[25] Salmon E.D, Cimini D, Cameron L.A, and DeLuca J.G. Merotelic kinetochores in mammalian tissue cells. Philosophical Transactions of the Royal Society B: Biological Sciences, 360(1455):553–568, March 2005.

[26] Cornelia Rumpf, Lubos Cipak, Alexander Schleiffer, Alison Pidoux, Karl Mechtler, Iva M. Tolić-Nørrelykke, and Juraj Gregan. Laser microsurgery provides evidence for merotelic kinetochore attachments in fission yeast cells lacking Pcs1 or Clr4. Cell Cycle, 9(19):3997–4004, October 2010.

[27] Juraj Gregan, Silvia Polakova, Lijuan Zhang, Iva M. Tolić-Nørrelykke, and Daniela Cimini. Merotelic kinetochore attachment: Causes and effects. Trends in Cell Biology, 21(6):374–381, June 2011.

[28] Michael A. Lampson and Ekaterina L. Grishchuk. Mechanisms to Avoid and Correct Erroneous Kinetochore-Microtubule Attachments. Biology, 6(1):1, January 2017.

[29] Carlos Sacristan and Geert J. P. L. Kops. Joined at the hip: Kinetochores, microtubules, and spindle assembly checkpoint signaling. Trends in Cell Biology, 25(1):21–28, January 2015.

[30] Juraj Gregan, Christian G. Riedel, Alison L. Pidoux, Yuki Katou, Cornelia Rumpf, Alexander Schleiffer, Stephen E. Kearsey, Katsuhiko Shirahige, Robin C. Allshire, and Kim Nasmyth. The Kinetochore Proteins Pcs1 and Mde4 and Heterochromatin Are Required to Prevent Merotelic Orientation. Current Biology, 17(14):1190–1200, July 2007.

[31] R. Paul, R. Wollman, W. T. Silkworth, I. K. Nardi, D. Cimini, and A. Mogilner. Computer simulations predict that chromosome movements and rotations accelerate mitotic spindle assembly without compromising accuracy. Proceedings of the National Academy of Sciences, 106(37):15708–15713, 2009.

[32] Valentin Magidson, Raja Paul, Nachen Yang, Jeffrey G. Ault, Christopher B. O'Connell, Irina Tikhonenko, Bruce F. McEwen, Alex Mogilner, and Alexey Khodjakov. Adaptive changes in the kinetochore architecture facilitate proper spindle assembly. Nature Cell Biology, 2015.

[33] Anatoly V. Zaytsev and Ekaterina L. Grishchuk. Basic mechanism for biorientation of mitotic chromosomes is provided by the kinetochore geometry and indiscriminate turnover of kinetochore microtubules. Molecular Biology of the Cell, 26(22):3985–3998, May 2015.

[34] Andrea Musacchio. The Molecular Biology of Spindle Assembly Checkpoint Signaling Dynamics. Current Biology, 25(20):R1002–R1018, October 2015.

[35] Edward D. Salmon and Kerry Bloom. Tension sensors reveal how the kinetochore shares its load. BioEssays, 39(7):1600216, July 2017.

[36] Natalie J. Nannas and Andrew W. Murray. Tethering Sister Centromeres to Each Other Suggests the Spindle Checkpoint Detects Stretch within the Kinetochore. PLOS Genetics, 10(8):e1004492, August 2014.

[37] Eric C. Tauchman, Frederick J. Boehm, and Jennifer G. DeLuca. Stable kinetochore–microtubule attachment is sufficient to silence the spindle assembly checkpoint in human cells. Nature Communications, 6, December 2015.

[38] Jonathan Kuhn and Sophie Dumont. Spindle assembly checkpoint satisfaction occurs via end-on but not lateral attachments under tension. J Cell Biol, 216(6):1533–1542, June 2017.

[39] Tae Yeon Yoo, Jeong-Mo Choi, William Conway, Che-Hang Yu, Rohit V Pappu, and Daniel J Needleman. Measuring NDC80 binding reveals the molecular basis of tension-dependent kinetochore-microtubule attachments. eLife, 7:e36392, July 2018.

[40] Iain M. Cheeseman, Scott Anderson, Miri Jwa, Erin M. Green, Jung-seog Kang, John R. Yates III, Clarence S. M. Chan, David G. Drubin, and Georjana Barnes. Phospho-Regulation of Kinetochore-Microtubule Attachments by the Aurora Kinase Ipl1p. Cell, 111(2):163–172, October 2002.

[41] Daniela Cimini, Xiaohu Wan, Christophe B. Hirel, and E. D. Salmon. Aurora Kinase Promotes Turnover of Kinetochore Microtubules to Reduce Chromosome Segregation Errors. Current Biology, 16(17):1711–1718, September 2006.

[42] Dan Liu, Gerben Vader, Martijn J. M. Vromans, Michael A. Lampson, and Susanne M. A. Lens. Sensing chromosome bi-orientation by spatial separation of aurora B kinase from kinetochore substrates. Science (New York, N.Y.), 323(5919):1350–1353, March 2009.

[43] Dan Liu, Mathijs Vleugel, Chelsea B. Backer, Tetsuya Hori, Tatsuo Fukagawa, Iain M. Cheeseman, and Michael A. Lampson. Regulated targeting of protein phosphatase 1 to the outer kinetochore by KNL1 opposes Aurora B kinase. The Journal of Cell Biology, page jcb.201001006, March 2010.

[44] Sophie Dumont and Timothy J. Mitchison. Force and Length in the Mitotic Spindle. Current Biology, 19(17):R749–R761, September 2009.

[45] Gohta Goshima and Jonathan M. Scholey. Control of Mitotic Spindle Length. Annual Review of Cell and Developmental Biology, 26(1):21–57, 2010.

[46] Natalie J. Nannas, Eileen T. O'Toole, Mark Winey, and Andrew W. Murray. Chromosomal attachments set length and microtubule number in the Saccharomyces cerevisiae mitotic spindle. Molecular Biology of the Cell, 25(25):4034–4048, December 2014.

[47] Rania S. Rizk, Katherine A. DiScipio, Kathleen G. Proudfoot, and Mohan L. Gupta. The kinesin-8 Kip3 scales anaphase spindle length by suppression of midzone microtubule polymerization. The Journal of Cell Biology, 204(6):965–975, March 2014.

[48] Benjamin Lacroix, Gaëlle Letort, Laras Pitayu, Jérémy Sallé, Marine Stefanutti, Gilliane Maton, Anne-Marie Ladouceur, Julie C. Canman, Paul S. Maddox, Amy S. Maddox, Nicolas Minc, François Nédélec, and Julien Dumont. Microtubule Dynamics Scale with Cell Size to Set Spindle Length and Assembly Timing. Developmental Cell, 45(4):496–511.e6, May 2018.

[49] William S. Saunders and M. Andrew Hoyt. Kinesin-related proteins required for structural integrity of the mitotic spindle. Cell, 70(3):451–458, August 1992.

[50] Viktoriya Syrovatkina, Chuanhai Fu, and Phong T. Tran. Antagonistic Spindle Motors and MAPs Regulate Metaphase Spindle Length and Chromosome Segregation. Current Biology, 23(23):2423–2429, December 2013.

[51] Jeremy M. Chacón, Soumya Mukherjee, Breanna M. Schuster, Duncan J. Clarke, and Melissa K. Gardner. Pericentromere tension is self-regulated by spindle structure in metaphase. The Journal of Cell Biology, 205(3):313–324, December 2014.

[52] Zachary R. Gergely, Ammon Crapo, Loren E. Hough, J. Richard McIntosh, and Meredith D. Betterton. Kinesin-8 effects on mitotic microtubule dynamics contribute to spindle function in fission yeast. Molecular Biology of the Cell, 27(22):3490–3514, July 2016.

[53] Scott V. Bratman and Fred Chang. Stabilization of Overlapping Microtubules by Fission Yeast CLASP. Developmental Cell, 13(6):812–827, December 2007.

[54] Karen Griffiths, Hirohisa Masuda, Susheela Dhut, and Takashi Toda. Fission yeast dam1-A8 mutant is resistant to and rescued by an anti-microtubule agent. Biochemical and Biophysical Research Communications, 368(3):670–676, April 2008.

[55] Sung Hugh Choi, Marie-Pierre Péli-Gulli, Iain Mcleod, Ali Sarkeshik, John R. Yates, Viesturs Simanis, and Dannel McCollum. Phosphorylation state defines discrete roles for monopolin in chromosome attachment and spindle elongation. Current biology: CB, 19(12):985–995, June 2009.

[56] Kuo-Shun Hsu and Takashi Toda. Ndc80 Internal Loop Interacts with Dis1/TOG to Ensure Proper Kinetochore-Spindle Attachment in Fission Yeast. Current Biology, 21(3):214–220, February 2011.

[57] Hirohisa Masuda, Risa Mori, Masashi Yukawa, and Takashi Toda. Fission yeast MOZART1/Mzt1 is an essential γ-tubulin complex component required for complex recruitment to the microtubule organizing center, but not its assembly. Molecular Biology of the Cell, 24(18):2894–2906, September 2013.

[58] Sarah Wälde and Megan C. King. The KASH protein Kms2 coordinates mitotic remodeling of the spindle pole body. J Cell Sci, 127(16):3625–3640, August 2014.

[59] Jonathan J. Ward, Hélio Roque, Claude Antony, and François Nédélec. Mechanical design principles of a mitotic spindle. eLife, 3:e03398, January 2015.

[60] Hadrien Mary, Jonathan Fouchard, Guillaume Gay, Céline Reyes, Tiphaine Gauthier, Clémence Gruget, Jacques Pécréaux, Sylvie Tournier, and Yannick Gachet. Fission yeast kinesin-8 controls chromosome congression independently of oscillations. J Cell Sci, 128(20):3720–3730, October 2015.

[61] Anna H. Klemm, Agneza Bosilj, Matko Gluncic, Nenad Pavin, and Iva M. Tolic. Metaphase kinetochore movements are regulated by kinesin-8 motors and microtubule dynamic instability. Molecular Biology of the Cell, 29(11):1332–1345, April 2018.

[62] Robert Blackwell, Oliver Sweezy-Schindler, Christopher Edelmaier, Zachary R. Gergely, Patrick J. Flynn, Salvador Montes, Ammon Crapo, Alireza Doostan, J. Richard McIntosh, Matthew A. Glaser, and Meredith D. Betterton. Contributions of Microtubule Dynamic Instability and Rotational Diffusion to Kinetochore Capture. Biophysical Journal, 112(3):552–563, February 2017.

[63] Robert Blackwell, Christopher Edelmaier, Oliver Sweezy-Schindler, Adam Lamson, Zachary R. Gergely, Eileen O'Toole, Ammon Crapo, Loren E. Hough, J. Richard McIntosh, Matthew A. Glaser, and Meredith D. Betterton. Physical determinants of bipolar mitotic spindle assembly and stability in fission yeast. Science Advances, 3(1):e1601603, January 2017.

[64] Matko Glunčić, Nicola Maghelli, Alexander Krull, Vladimir Krstić, Damien Ramunno-Johnson, Nenad Pavin, and Iva M. Tolić. Kinesin-8 Motors Improve Nuclear Centering by Promoting Microtubule Catastrophe. Physical Review Letters, 114(7):078103, February 2015.

[65] Adam R. Lamson, Christopher J. Edelmaier, Matthew A. Glaser, and Meredith D. Betterton. Theory of Cytoskeletal Reorganization during Cross-Linker-Mediated Mitotic Spindle Assembly. Biophysical Journal, 116(9):1719–1731, May 2019.

[66] Sergio A. Rincon, Adam Lamson, Robert Blackwell, Viktoriya Syrovatkina, Vincent Fraisier, Anne Paoletti, Meredith D. Betterton, and Phong T. Tran. Kinesin-5-independent mitotic spindle assembly requires the antiparallel microtubule crosslinker Ase1 in fission yeast. Nature Communications, 8:15286, May 2017.

[67] Ingrid Brust-Mascher, Gul Civelekoglu-Scholey, and Jonathan M. Scholey. Mechanism for Anaphase B: Evaluation of "Slide-and-Cluster" versus "Slide-and-Flux-or-Elongate" Models. Biophysical Journal, 108(8):2007–2018, April 2015.

[68] D. Johann, D. Goswami, and K. Kruse. Generation of Stable Overlaps between Antiparallel Filaments. Physical Review Letters, 115(11):118103, September 2015.

[69] D. Johann, D. Goswami, and K. Kruse. Assembly of bipolar microtubule structures by passive cross-linkers and molecular motors. Physical Review E, 93(6):062415, June 2016.

[70] Rui Ma, Liedewij Laan, Marileen Dogterom, Nenad Pavin, and Frank Jülicher. General theory for the mechanics of confined microtubule asters. New Journal of Physics, 16(1):013018, January 2014.

[71] Carlos Garzon-Coral, Horatiu A. Fantana, and Jonathon Howard. A force-generating machinery maintains the spindle at the cell center during mitosis. Science, 352(6289):1124–1127, May 2016.

[72] Jan Brugués and Daniel Needleman. Physical basis of spindle self-organization. Proceedings of the National Academy of Sciences, 111(52):18496–18500, December 2014.

[73] Maja Novak, Bruno Polak, Juraj Simunić, Zvonimir Boban, Barbara Kuzmić, Andreas W. Thomae, Iva M. Tolić, and Nenad Pavin. The mitotic spindle is chiral due to torques within microtubule bundles. Nature Communications, 9(1):3571, September 2018.

[74] Stefanie Redemann, Johannes Baumgart, Norbert Lindow, Michael Shelley, Ehssan Nazockdast, Andrea Kratz, Steffen Prohaska, Jan Brugués, Sebastian Fürthauer, and Thomas Müller-Reichert. C. elegans chromosomes connect to centrosomes by anchoring into the spindle network. Nature Communications, 8:15288, May 2017.

[75] Lora Winters, Ivana Ban, Marcel Prelogovic, Nenad Pavin, and Iva M. Tolic. Pivoting of microtubules driven by minus end directed motors leads to their alignment to form an interpolar bundle. bioRxiv, page 347831, June 2018.

[76] Iana Kalinina, Amitabha Nandi, Petrina Delivani, Mariola R. Chacón, Anna H. Klemm, Damien Ramunno-Johnson, Alexander Krull, Benjamin Lindner, Nenad Pavin, and Iva M. Tolić-Norrelykke. Pivoting of microtubules around the spindle pole accelerates kinetochore capture. Nature Cell Biology, 2012.

[77] Emily S. Tubman, Sue Biggins, and David J. Odde. Stochastic Modeling Yields a Mechanistic Framework for Spindle Attachment Error Correction in Budding Yeast Mitosis. Cell Systems, 4(6):645–650.e5, June 2017.

[78] Prasad Trivedi, Anatoly V. Zaytsev, Maxim Godzi, Fazly I. Ataullakhanov, Ekaterina L. Grishchuk, and P. Todd Stukenberg. The binding of Borealin to microtubules underlies a tension independent kinetochore-microtubule error correction pathway. Nature Communications, 10(1):682, February 2019.

[79] Edward J. Banigan, Kevin K. Chiou, Edward R. Ballister, Alyssa M. Mayo, Michael A. Lampson, and Andrea J. Liu. Minimal model for collective kinetochore–microtubule dynamics. Proceedings of the National Academy of Sciences, 112(41):12699–12704, October 2015.

[80] Kruno Vukušić, Renata Buđa, Agneza Bosilj, Ana Milas, Nenad Pavin, and Iva M. Tolić. Microtubule Sliding within the Bridging Fiber Pushes Kinetochore Fibers Apart to Segregate Chromosomes. Developmental Cell, 43(1):11–23.e6, October 2017.

[81] Tong Gao, Robert Blackwell, Matthew A. Glaser, Meredith Betterton, and Michael J. Shelley. Multiscale Polar Theory of Microtubule and Motor-Protein Assemblies. Physical Review Letters, 114(4):048101, January 2015.

[82] Tong Gao, Robert Blackwell, Matthew A. Glaser, M. D. Betterton, and Michael J. Shelley. Multiscale modeling and simulation of microtubule-motor-protein assemblies. Physical Review E, 92(6):062709, December 2015.

[83] Robert Blackwell, Oliver Sweezy-Schindler, Christopher Baldwin, Loren E. Hough, Matthew A. Glaser, and M. D. Betterton. Microscopic origins of anisotropic active stress in motor-driven nematic liquid crystals. Soft Matter, 12:2676–2687, January 2016.

[84] Masaki Edamatsu. Bidirectional motility of the fission yeast kinesin-5, Cut7. Biochemical and Biophysical Research Communications, 446(1):231–234, March 2014.

[85] M. Edamatsu. Molecular properties of the N-terminal extension of the fission yeast kinesin-5, Cut7. Genetics and molecular research : GMR, 15(1), February 2016.

[86] Mishan Britto, Adeline Goulet, Syeda Rizvi, Ottilie von Loeffelholz, Carolyn A. Moores, and Robert A. Cross. Schizosaccharomyces pombe kinesin-5 switches direction using a steric blocking mechanism. Proceedings of the National Academy of Sciences, page 201611581, November 2016.

[87] Sudhir Kumar Singh, Himanshu Pandey, Jawdat Al-Bassam, and Larisa Gheber. Bidirectional motility of kinesin-5 motor proteins: Structural determinants, cumulative functions and physiological roles. Cellular and Molecular Life Sciences, 75(10):1757–1771, May 2018.

[88] Cynthia L. Troxell, Mark A. Sweezy, Robert R. West, Karen D. Reed, Bryan D. Carson, Alison L. Pidoux, W. Zacheus Cande, and J. Richard McIntosh. Pkl1 +andklp2 +: Two Kinesins of the Kar3 Subfamily in Fission Yeast Perform Different Functions in Both Mitosis and Meiosis. Molecular Biology of the Cell, 12(11):3476–3488, January 2001.

[89] Zachary T. Olmsted, Andrew G. Colliver, Timothy D. Riehlman, and Janet L. Paluh. Kinesin-14 and kinesin-5 antagonistically regulate microtubule nucleation by γ-TuRC in yeast and human cells. Nature Communications, 5:5339, October 2014.

[90] Masashi Yukawa, Chiho Ikebe, and Takashi Toda. The Msd1–Wdr8–Pkl1 complex anchors microtubule minus ends to fission yeast spindle pole bodies. J Cell Biol, 209(4):549–562, May 2015.

[91] Masashi Yukawa, Yusuke Yamada, Tomoaki Yamauchi, and Takashi Toda. Two spatially distinct Kinesin-14 Pkl1 and Klp2 generate collaborative inward forces against Kinesin-5 Cut7 in S. pombe. J Cell Sci, page jcs.210740, January 2017.

[92] Isabelle Loïodice, Jayme Staub, Thanuja Gangi Setty, Nam-Phuong T. Nguyen, Anne Paoletti, and P. T. Tran. Ase1p Organizes Antiparallel Microtubule Arrays during Interphase and Mitosis in Fission Yeast. Molecular Biology of the Cell, 16(4):1756–1768, January 2005.

[93] Lukas C. Kapitein, Marcel E. Janson, Siet M. J. L. van den Wildenberg, Casper C. Hoogenraad, Christoph F. Schmidt, and Erwin J. G. Peterman. Microtubule-Driven Multimerization Recruits ase1p onto Overlapping Microtubules. Current Biology, 18(21):1713–1717, November 2008.

[94] Thibault Courtheoux, Guillaume Gay, Yannick Gachet, and Sylvie Tournier. Ase1/Prc1-dependent spindle elongation corrects merotely during anaphase in fission yeast. The Journal of Cell Biology, 187(3):399–412, February 2009.

[95] Chuanhai Fu, Jonathan J. Ward, Isabelle Loiodice, Guilhem Velve-Casquillas, Francois J. Nedelec, and Phong T. Tran. Phospho-Regulated Interaction between Kinesin-6 Klp9p and Microtubule Bundler Ase1p Promotes Spindle Elongation. Developmental Cell, 17(2):257–267, August 2009.

[96] R. Ding, K. L. McDonald, and J. R. McIntosh. Three-dimensional reconstruction and analysis of mitotic spindles from the yeast, Schizosaccharomyces pombe. The Journal of Cell Biology, 120(1):141–151, January 1993.

[97] Bungo Akiyoshi, Krishna K. Sarangapani, Andrew F. Powers, Christian R. Nelson, Steve L. Reichow, Hugo Arellano-Santoyo, Tamir Gonen, Jeffrey A. Ranish, Charles L. Asbury, and Sue Biggins. Tension directly stabilizes reconstituted kinetochore-microtubule attachments. Nature, 468(7323):576–579, November 2010.

[98] Matthew P. Miller, Charles L. Asbury, and Sue Biggins. A TOG Protein Confers Tension Sensitivity to Kinetochore-Microtubule Attachments. Cell, 165(6):1428–1439, June 2016.

[99] Y. Yamagishi, C. H. Yang, Y. Tanno, and Y. Watanabe. MPS1/Mph1 phosphorylates the kinetochore protein KNL1/Spc7 to recruit SAC components. Nature Cell Biology, 14(7):746–752, 2012.

[100] Ayumu Yamamoto and Yasushi Hiraoka. Monopolar spindle attachment of sister chromatids is ensured by two distinct mechanisms at the first meiotic division in fission yeast. The EMBO Journal, 22(9):2284–2296, May 2003.

[101] Guillaume Gay, Thibault Courtheoux, Céline Reyes, Sylvie Tournier, and Yannick Gachet. A stochastic model of kinetochore–microtubule attachment accurately describes fission yeast chromosome segregation. The Journal of Cell Biology, 196(6):757–774, March 2012.

[102] Khuloud Jaqaman, Dinah Loerke, Marcel Mettlen, Hirotaka Kuwata, Sergio Grinstein, Sandra L. Schmid, and Gaudenz Danuser. Robust single-particle tracking in live-cell time-lapse sequences. Nature Methods, 5(8):695–702, August 2008.

[103] E. L. Grishchuk and J. R. McIntosh. Microtubule depolymerization can drive poleward chromosome motion in fission yeast. The EMBO Journal, 25(20):4888–4896, 2006.

[104] J. Richard McIntosh, Eileen O'Toole, Kirill Zhudenkov, Mary Morphew, Cindi Schwartz, Fazly I. Ataullakhanov, and Ekaterina L. Grishchuk. Conserved and divergent features of kinetochores and spindle microtubule ends from five species. The Journal of Cell Biology, 200(4):459–474, February 2013.

[105] Jennifer G. DeLuca, Walter E. Gall, Claudio Ciferri, Daniela Cimini, Andrea Musacchio, and E. D. Salmon. Kinetochore Microtubule Dynamics and Attachment Stability Are Regulated by Hec1. Cell, 127(5):969–982, December 2006.

[106] A. Franco, J. C. Meadows, and J. B. A. Millar. The Dam1/DASH complex is required for the retrieval of unclustered kinetochores in fission yeast. Journal of Cell Science, 120(19):3345–3351, 2007.

[107] Yannick Gachet, Céline Reyes, Thibault Courthéoux, Sherilyn Goldstone, Guillaume Gay, Céline Serrurier, and Sylvie Tournier. Sister Kinetochore Recapture in Fission Yeast Occurs by Two Distinct Mechanisms, Both Requiring Dam1 and Klp2. Molecular Biology of the Cell, 19(4):1646–1662, January 2008.

[108] Qi Gao, Thibault Courtheoux, Yannick Gachet, Sylvie Tournier, and Xiangwei He. A non-ring-like form of the Dam1 complex modulates microtubule dynamics in fission yeast. Proceedings of the National Academy of Sciences, 107(30):13330–13335, July 2010.

[109] Iain Hagan and Mitsuhiro Yanagida. Novel potential mitotic motor protein encoded by the fission yeast cut7+ gene. Nature, 347(6293):563–566, October 1990.

[110] Iain Hagan and Mitsuhiro Yanagida. Kinesin-related cut 7 protein associates with mitotic and meiotic spindles in fission yeast. Nature, 356(6364):74, March 1992.

[111] Takashi Toda, Masashi Yukawa, and Yusuke Yamada. Suppressor analysis uncovers that MAPs and microtubule dynamics balance with the Cut7/Kinesin-5 motor for mitotic spindle assembly in Schizosaccharomyces pombe. bioRxiv, page 380493, July 2018.

[112] Daniela Cimini, Ben Moree, Julie C. Canman, and E. D. Salmon. Merotelic kinetochore orientation occurs frequently during early mitosis in mammalian tissue cells and error correction is achieved by two different mechanisms. Journal of Cell Science, 116(20):4213–4225, October 2003.

[113] R. Bruce Nicklas and Carol A. Koch. CHROMOSOME MICROMANIPULATION: III. Spindle Fiber Tension and the Reorientation of Mal-Oriented Chromosomes. The Journal of Cell Biology, 43(1):40–50, October 1969.

[114] Kentaro Nabeshima, Takashi Nakagawa, Aaron F. Straight, Andrew Murray, Yuji Chikashige, Yukiko M. Yamashita, Yasushi Hiraoka, and Mitsuhiro Yanagida. Dynamics of Centromeres during Metaphase–Anaphase Transition in Fission Yeast: Dis1 Is Implicated in Force Balance in Metaphase Bipolar Spindle. Molecular Biology of the Cell, 9(11):3211–3225, January 1998.

[115] Gohta Goshima, Shigeaki Saitoh, and Mitsuhiro Yanagida. Proper metaphase spindle length is determined by centromere proteins Mis12 and Mis6 required for faithful chromosome segregation. Genes & Development, 13(13):1664–1677, January 1999.

[116] Fedor Severin, Bianca Habermann, Tim Huffaker, and Tony Hyman. Stu2 Promotes Mitotic Spindle Elongation in Anaphase. The Journal of Cell Biology, 153(2):435–442, April 2001.

[117] Iva Marija Tolić-Nørrelykke, Emilia-Laura Munteanu, Genevieve Thon, Lene Oddershede, and Kirstine Berg-Sørensen. Anomalous Diffusion in Living Yeast Cells. Physical Review Letters, 93(7):078102, August 2004.

[118] David C. Bouck and Kerry Bloom. Pericentric Chromatin Is an Elastic Component of the Mitotic Spindle. Current Biology, 17(9):741–748, May 2007.

[119] Andrew D. Stephens, Rachel A. Haggerty, Paula A. Vasquez, Leandra Vicci, Chloe E. Snider, Fu Shi, Cory Quammen, Christopher Mullins, Julian Haase, Russell M. Taylor, Jolien S. Verdaasdonk, Michael R. Falvo, Yuan Jin, M. Gregory Forest, and Kerry Bloom. Pericentric chromatin loops function as a nonlinear spring in mitotic force balance. The Journal of Cell Biology, 200(6):757–772, March 2013.

[120] Judite Costa, Chuanhai Fu, V. Mohini Khare, and Phong T. Tran. Csi2p modulates microtubule dynamics and organizes the bipolar spindle for chromosome segregation. Molecular Biology of the Cell, pages mbc.E14–09–1370, September 2014.

[121] Fan Zheng, Tianpeng Li, Dong-yan Jin, Viktoriya Syrovatkina, Kathleen Scheffler, Phong T. Tran, and Chuanhai Fu. Csi1p recruits alp7p/TACC to the spindle pole bodies for bipolar spindle formation. Molecular Biology of the Cell, 25(18):2750–2760, September 2014.

[122] Roy G. H. P. van Heesbeen, Marvin E. Tanenbaum, and René H. Medema. Balanced Activity of Three Mitotic Motors Is Required for Bipolar Spindle Assembly and Chromosome Segregation. Cell Reports, 8(4):948–956, August 2014.

[123] Viktoriya Syrovatkina and Phong T. Tran. Loss of kinesin-14 results in aneuploidy via kinesin-5-dependent microtubule protrusions leading to chromosome cut. Nature Communications, 6:7322, June 2015.

[124] Melissa K. Gardner, Chad G. Pearson, Brian L. Sprague, Ted R. Zarzar, Kerry Bloom, E. D. Salmon, and David J. Odde. Tension-dependent Regulation of Microtubule Dynamics at Kinetochores Can Explain Metaphase Congression in Yeast. Molecular Biology of the Cell, 16(8):3764–3775, January 2005.

[125] Melissa K. Gardner, David J. Odde, and Kerry Bloom. Kinesin-8 molecular motors: Putting the brakes on chromosome oscillations. Trends in Cell Biology, 18(7):307–310, July 2008.

[126] E.N. Cytrynbaum, J.M. Scholey, and A. Mogilner. A Force Balance Model of Early Spindle Pole Separation in Drosophila Embryos. Biophysical Journal, 84(2):757–769, February 2003.

[127] E. N. Cytrynbaum, P. Sommi, I. Brust-Mascher, J. M. Scholey, and A. Mogilner. Early Spindle Assembly in Drosophila Embryos: Role of a Force Balance Involving Cytoskeletal Dynamics and Nuclear Mechanics. Molecular Biology of the Cell, 16(10):4967–4981, January 2005.

[128] Roy Wollman, Gul Civelekoglu-Scholey, Jonathan M Scholey, and Alex Mogilner. Reverse engineering of force integration during mitosis in the Drosophila embryo. Molecular Systems Biology, 4, May 2008.

[129] Gul Civelekoglu-Scholey and Jonathan M. Scholey. Mitotic force generators and chromosome segregation. Cellular and Molecular Life Sciences, 67(13):2231–2250, July 2010.

[130] Yuta Shimamoto, Scott Forth, and Tarun M. Kapoor. Measuring Pushing and Braking Forces Generated by Ensembles of Kinesin-5 Crosslinking Two Microtubules. Developmental Cell, 34(6):669–681, September 2015.

[131] Christian Hentrich and Thomas Surrey. Microtubule organization by the antagonistic mitotic motors kinesin-5 and kinesin-14. The Journal of Cell Biology, 189(3):465–480, March 2010.

[132] J. C. Waters, T. J. Mitchison, C. L. Rieder, and E. D. Salmon. The kinetochore microtubule minus-end disassembly associated with poleward flux produces a force that can do work. Molecular Biology of the Cell, 7(10):1547–1558, January 1996.

[133] R. Bruce Nicklas. How Cells Get the Right Chromosomes. Science, 275(5300):632–637, January 1997.